frontiers | Frontiers in Environmental Science

TYPE Original Research
PUBLISHED 08 January 2024
DOI 10.3389/fenvs.2023.1341017

OPEN ACCESS

EDITED BY
Ming Zhong,
Sun Yat-sen University, China

REVIEWED BY
Changqing Meng,
North China Electric Power University, China
Yong Tian,
Southern University of Science and Technology, China
Shuo Ouyang,
Changjiang Water Resources Commission, China

*CORRESPONDENCE
Junxiang Liu,
jx.liu.csg@hotmail.com

RECEIVED 19 November 2023
ACCEPTED 15 December 2023
PUBLISHED 08 January 2024

CITATION
Liu J, Hong H, Fan W and Chen Y (2024), A novel fast and efficient adaptive shuffled complex evolution algorithm for model parameter calibration.
Front. Environ. Sci. 11:1341017.
doi: 10.3389/fenvs.2023.1341017

A novel fast and efficient adaptive shuffled complex evolution algorithm for model parameter calibration

Junxiang Liu*, Haicheng Hong, Weinan Fan and Yilong Chen

Guangdong Power Grid Co., Ltd., Guangzhou, China

The research and optimization of hydrological forecasting models are among the most crucial components in the scope of water management and flood protection. Optimizing the calibration of hydrological forecasting models is crucial for forecasting performance. A rapid adaptive Shuffled Complex Evolution (SCE) method called Fast Adaptive SCE (FASCE) is proposed for calibrating model parameters. It builds upon the previously established SCE-UA, known for its effectiveness and robustness in the same calibration context. The robustness of the original SCE-UA is expanded upon, introducing a revised adaptive simplex search to bolster efficiency. Additionally, a new strategy for setting up the initial population base enhances explorative capacities. FASCE's performance has been assessed alongside numerous methods from prior studies, demonstrating its effectiveness. Initial tests were conducted on a set of functions to assess FASCE's efficacy. Findings revealed that FASCE could curtail the failure rate by a minimum of 80%, whereas the requirement for function evaluations fell between 30% and 60%. Two hydrological models - Support Vector Machine (SVM) and Xinanjiang rainfall-runoff model were employed to estimate the new algorithm's performance. No failures were reported, and there was a reduction of at least 30% in function evaluations using FASCE. The outcomes from these studies affirm that FASCE can considerably reduce both the number of failures and the count of function evaluations required to reach the global maximum. Hence, FASCE emerges as a viable substitute for model parameter calibration.

KEYWORDS

model calibration, adaptive shuffle, support vector machine, hydrological model, streamflow forcasting

1 Introduction

The research and optimization of hydrological forecasting models are among the most crucial components in the scope of water management and flood protection. In hydrological forecasting research, a key component involves calibrating parameters of streamflow forecasting models. Accurate forecasts of streamflow are crucial as they furnish vital information for supporting reservoirs' optimal operation and ensuring control over flood processes (Qin et al., 2010; Chen et al., 2013; 2016; Ouyang et al., 2013; Tsai et al., 2014; Yazdi et al., 2014; Li and Ouyang, 2015; Zhou et al., 2015).

Over the past several decades, scientists in the field have crafted numerous algorithms for calibration. One standout amidst these is Duan et al. (1992) Shuffled Complex Evolution Algorithm (SCE-UA). Known for its robustness and efficiency, through myriad successful applications, it has established itself as a reliable global optimization method for calibrating model parameters (Duan et al., 1992; Yapo et al., 1996; Santos et al., 2003; Ajami et al., 2004; He et al., 2007; Mcmillan et al., 2010; Liu et al., 2015; Uniyal et al., 2015; Her and Heatwole, 2016; Yang J. et al., 2017a; Gopala et al., 2019; Hallabia et al., 2021; Brunetti et al., 2022; Guo et al., 2023). Notably, SCE-UA and related derivatives also target multi-objective optimization problems, extending applications to groundwater and reservoir models (Muttil and Jayawardena, 2008; Chu et al., 2014; Yang et al., 2015; Yang T. et al., 2017b).

Past studies indicate that population diversity greatly impacts the search performance of algorithms (Bremermann et al., 1966; Galar, 1985; Fogel et al., 1998; Muttil and Liong, 2004). Yet, SCE-UA creates populations in a purely random manner. Under certain circumstances, this may inhibit SCE-UA's convergence to the global optimum. Further constraining SCE-UA's efficiency, it only spawns new individuals based on the poorest individual and the centroid of the remaining individuals, failing to fully harness previously obtained optimal results data.

Addressing these shortcomings, this research introduces the Fast Adaptive Shuffled Complex Evolution (FASCE), an algorithm based on SCE-UA that heightens the search efficiency through an adaptive simplex search, replacing SCE-UA's original simplex search. The initial population's placement strategy, as proposed by Muttil and Jayawardena (2008), is also merged to boost the algorithm's exploratory capabilities.

FASCE's effectiveness was validated through various benchmark functions and two daily streamflow forecasting models grounded on Support Vector Machine (SVM) and Xinanjiang model. Due to its excellent performance, SVM is extensively utilized and have been successfully implemented in the field of hydrology (Lin et al., 2006; Tripathi et al., 2006; Mohsen et al., 2009; Yoon et al., 2010; Kisi and Cimen, 2011; Yan et al., 2022; Xu et al., 2023). And the Xinanjiang model has been employed for streamflow forecasting during the last decades (Zhao, 1992; Zhao et al., 1995; Li et al., 2009; Song et al., 2012; Mao et al., 2013; Deng et al., 2015; Rahman and Lu, 2015; Jiang et al., 2023). FASCE's performance was compared with both the original SCE-UA and the enhanced SCE-UA algorithm (SCE-MJ), as proposed by Muttil and Jayawardena (2008). Results showed FASCE outperforming both and, as such, it stands as a promising alternative for model parameter calibration.

Our study aims to present a new and expedient adaptive shuffled complex evolution (SCE) algorithm for the calibration of streamflow forecasting models based on SVM and Xinanjiang rainfall-runoff model. Multiple search strategies that build upon the original SCE-UA algorithm have been introduced in this research. These innovative strategies enhance the algorithm's exploration capability and significantly improve its convergence speed. Our approach provides a fast and efficient solution for accurate calibration and forecasting in streamflow analysis.

2 Materials and methods

2.1 Description of the SCE-UA and SCE-MJ algorithm

The Shuffled Complex Evolution-University of Arizona (SCE-UA) algorithm is a powerful optimization method commonly used in hydrological and environmental modeling. It's based on the idea of simulating the complex behavior of nature's evolutionary process.

By imitating the natural evolution, SCE-UA algorithm efficiently explores a wide range of solution space to find the optimal solution for complex problems such as parameter calibration, uncertainty analysis, and sensitivity analysis. It has been applied in various fields like water resources management, climate modeling, and ecosystem analysis.

And the algorithm proposed by Muttil and Jayawardena (2008), called SCE-MJ model calibrating algorithm, aims to enhance robustness and efficiency in hydrological processes. It utilizes a shuffled complex approach, which involves multiple complexes, each with a set of parameters.

The SCE-MJ algorithm dynamically shuffles the parameter sets between complexes to explore the search space more effectively. This helps in finding the optimal parameter values for calibrating hydrological models. By introducing a crossover process and parameter adaptation, the algorithm improves the efficiency of the optimization process.

2.2 Design of FASCE based on SCE-UA and SCE-MJ

The FASCE process is a refined advancement over its predecessor, the SCE-UA method. Detailed comprehension of the SCE-UA model can be acquired through references such as Duan et al., 1992, Duan and Gupta, 1993; Li et al., 2013.

A strategic method offered by Muttil and Jayawardena in 2008 is adopted for determining the initial population in our research. This is geared towards ensuring the SCE-UA algorithm does not become trapped in the local optimality within feasible spatial dimensions. The said strategy is imperative in preserving diversity within the population group. Interested parties can gain more knowledge on this strategy by referring to Muttil and Jayawardena 2008.

Moreover, to elevate the potency of the algorithm's search capabilities, an innovative, adaptive simplex search mechanism is introduced within this study. This operator is utilized during the reflection or contraction phases to instigate the inception of a new point and shift adaptively towards the optimal point amidst the simplex.

This adaptive procedure is a significant enhancement against the standard SCE-UA method. Benefits include the ability to employ both the optimal point's data and the information derived during the process of generation. The advent of novel points, courtesy of this adaptive simplex search operator, is dictated by Eqs 1–4.

$$X_{new} = \theta X_b + (1 - \theta) X_{ref} \tag{1}$$

$$X_{new} = \theta X_b + (1 - \theta) X_{con} \tag{2}$$

$$S = \frac{1}{\bar{y}} \sqrt{\frac{1}{n} \sum_{i=1}^{n} (y_i - \bar{y})^2} \tag{3}$$

$$\theta = \begin{cases} \frac{1}{\sqrt{2\pi}} e^{-\frac{S^2}{2}}, & S > 0.05 \\ S, & S \le 0.05 \end{cases} \tag{4}$$

Where X_{new} denotes the new point, X_{ref} denotes the reflected point, X_{con} denotes the contracted point, X_b is the best point of the simplex, θ is the adaptive shift coefficient, n is the number of current population excluding the worst point, y_i is the objective function value of the ith point, $\bar{y}$ is the mean objective function value of the current population excluding the worst point, S denotes the fluctuation degree of the current population excluding the worst point.

Besides, the FASCE also uses two stopping criteria: Parameters distribution and Maximum number of function evaluation, which are the same with SCE-UA. This means that the algorithm can early stop when the parameters distribution is too narrow to search.

2.3 The differences between FASCE and SCE-MJ

In the SCE-MJ algorithm, the shift coefficient must be preset in advance. And this coefficient is always determined by artificial experience. Generally, for some relatively simple test functions (such as Goldstein-Price function, Six-hump function, Griewank function, and so on), the number of local optima is small, and the shift coefficient is set bigger, the shuffle operator can make the generated new point move fast to the global optimum, and the convergence speed is enhanced significantly; and for some complicated test functions (such as Restrigin function, Rastrigin (10D) function, Rosenbrock (10D) function, and so on), the number of local optima is relatively large, and the shift coefficient is set smaller. Thus, to avoid missing the global optimum, the shuffle operator can make the generated new point move slowly to the global optimum, and then the convergence speed improvement becomes small relatively.

However, the complexity of practical problems in engineering usually is not known. Therefore, it is very difficult to set reasonable shift coefficient. Besides, it is not reasonable to set a constant shift coefficient during the whole evolutionary computation process of the algorithm.

To overcome these shortcomings, we propose a novel algorithm FASCE with an adaptive shift operator. And this adaptive shift operator has no parameter needed predefined beforehand and can set adaptive shift coefficient according to the evolutionary computation process. There are three stage in the algorithm evolution as follows:

(1) At the initial stage of evolution, the fluctuation degree of the population is usually big. Then, the adaptive shift operator adopts small shift coefficient to avoid the algorithm missing global optimum.
(2) Meanwhile, with the evolution of algorithms, the fluctuation degree of the population is getting smaller and smaller, this indicates that the algorithm may be getting close to the final global optimum. At this situation, the adaptive shift operator gets big shift coefficient to make the algorithm converge fast to the global optimum.
(3) At the end of the algorithm evolution, the fluctuation degree of the population is getting very small. At this situation, the adaptive shift operator sets small shift coefficient to improve the search accuracy of algorithm.

The differences between these three algorithms are shown in Figure 1.

3 Benchmark functions testing results

In this study, eight widely recognized benchmark functions, denoted as Eqs 5–12, are utilized to evaluate the efficacy of the FASCE algorithm. These benchmark functions serve as valuable tools in gauging the performance and capabilities of the algorithm. By employing these benchmarks, we can comprehensively assess the algorithm's effectiveness and ascertain its potential for various applications.

(1) Restrigin function (dimension N = 2)

$$\begin{aligned} &f(x_1,x_2) = \sum_{i=1}^{2}\left[x_i^2 - 10\cos(2\pi x_i) + 10\right], x_1, x_2 \in [-5.12, 5.12] \\ &\min\left(f(x_1,x_2)\right) = f(0,0) = 0 \end{aligned} \tag{5}$$

(2) Goldstein-Price function (dimension N = 2)

$$\begin{aligned} &f(x_1,x_2) = \left[-2 + (x_1+x_2+1)^2\left(19 - 14x_1 + 3x_1^2 - 14x_2 + 6x_1x_2^2 + 3x_2^2\right)\right] \\ &\quad \times \left[30 + (2x_1 - 3x_2)^2\left(18 - 32x_1 + 12x_2^2 + 48x_2 - 36x_1x_2 + 27x_2^2\right)\right], \\ &x_1, x_2 \in [-2,2] \\ &\min\left(f(x_1,x_2)\right) = f(0,-1) = 0 \end{aligned} \tag{6}$$

(3) Rosenbrock function (dimension N = 2)

$$\begin{aligned} &f(x_1,x_2) = 100\left(x_2 - x_1^2\right) + \left(1 - x_1^2\right)^2, x_1 \in [-5,5], x_1 \in \left[-2,8\right) \\ &\min\left(f(x_1,x_2)\right) = f(1,1) = 0 \end{aligned} \tag{7}$$

(4) Griewank function (dimension N = 2)

$$\begin{aligned} &f(x_1,x_2) = \sum_{i=1}^{2}\frac{x_i^2}{d} - \prod_{i=1}^{2}\cos\left(\frac{x_i}{\sqrt{i}}\right) + 1, x_1, x_2 \in [-600,600], d = 600 \\ &\min\left(f(x_1,x_2)\right) = f(0,0) = 0 \end{aligned} \tag{8}$$

(5) Six-Hump function

$$\begin{aligned} &f(x_1,x_2) = 1.0316285 + 4x_1^2 - 2.1x_1^4 + \frac{1}{3}x_1^6 + x_1x_2 - 4x_2^2 + 4x_2^4, \\ &x_1 \in [-2,2], x_2 \in [-1,1] \\ &\min\left(f(x_1,x_2)\right) = f(0.08983,-0.7126) = f(-0.08983,0.7126) = 0 \end{aligned} \tag{9}$$

(6) Restrigin function (dimension $N = 10$)

$$\begin{aligned} &f(x_1,x_2,\cdots,x_{10}) = \sum_{i=1}^{10}\left[x_i^2 - 10\cos(2\pi x_i) + 10\right], x_i \in [-5.12, 5.12] \\ &\min\left(f(x_1,x_2,\cdots,x_{10})\right) = f(0,0,\cdots,0) = 0 \end{aligned} \tag{10}$$

(7) Rosenbrock function (dimension $N = 10$)

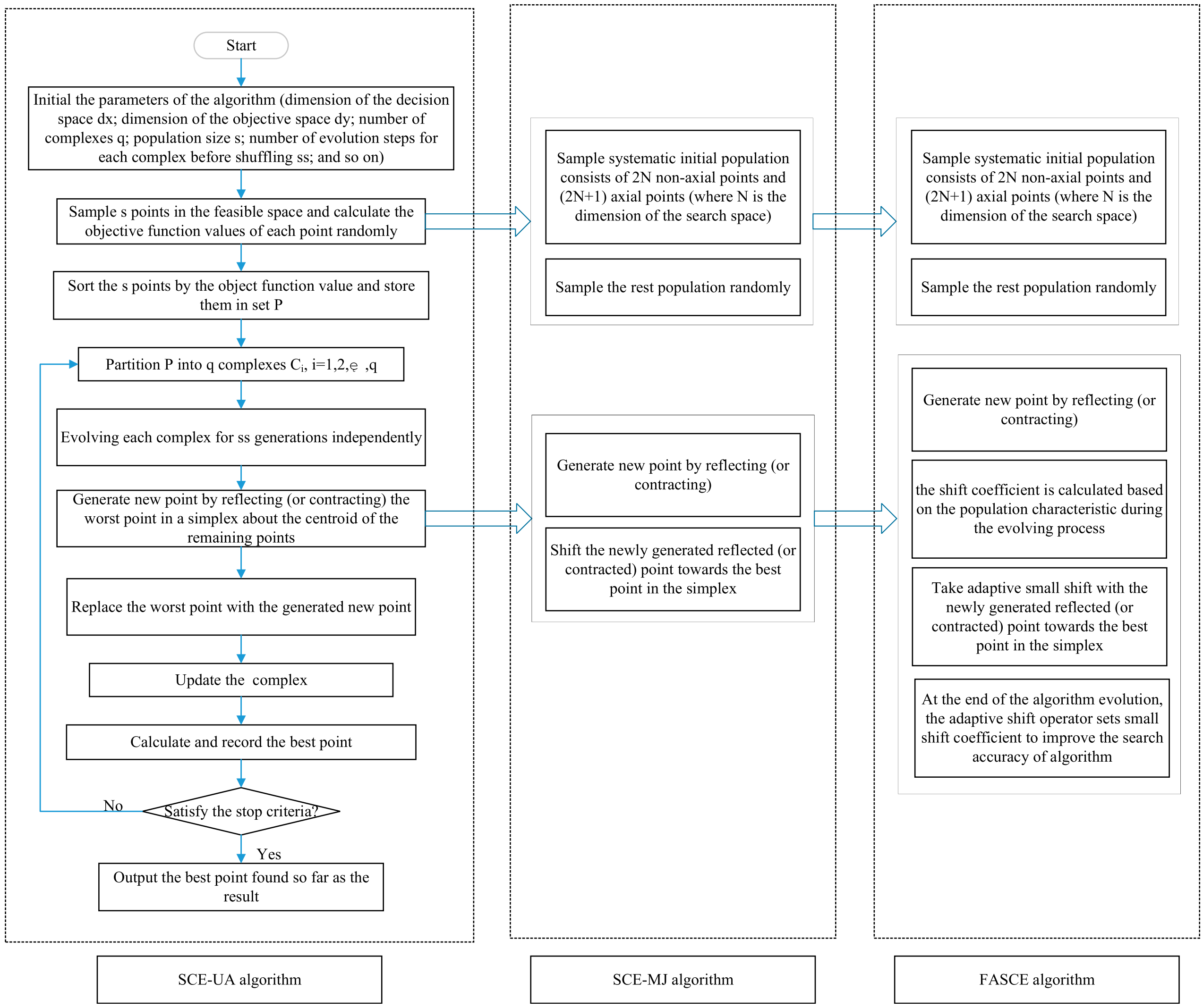

FIGURE 1
The flowchart of FASCE algorithm.

$$f(x_1, x_2, \cdots, x_{10}) = \sum_{i=1}^{9}\left[100\left(x_{i+1} - x_i^2\right)^2 + (1 - x_i)^2\right], |x_i| \le 30$$
$$\min\left(f(x_1, x_2 \cdots, x_{10})\right) = f(1, 1, \cdots, 1) = 0 \tag{11}$$

(8) Griewank function (dimension $N = 10$)

$$f(x_1, x_2, \cdots, x_{10}) = \sum_{i=1}^{10}\frac{x_i^2}{4000} - \prod_{i=1}^{10}\cos\left(\frac{x_i}{\sqrt{i}}\right) + 1, x_i \in [-600, 600],$$
$$\min\left(f(x_1, x_2, \cdots, x_{10})\right) = f(0, 0, \cdots, 0) = 0 \tag{12}$$

In order to assess the algorithm's performance, we utilize two indices: (a) the number of failures (NF) out of 100 trials and (b) the average number of function evaluations (NFE) for successful trials. Smaller values for NF and NFE indicate better performance. For this analysis, the maximum number of function evaluations is set to 25,000. A trial is deemed successful if the algorithm discovers a function value below 10^{-3} or is considered a failure if it reaches the maximum number of function evaluations.

Table 1 provides an overview of the outcomes from the FASCE algorithm. Additionally, to facilitate comparison, the results from both the original SCE-UA algorithm and the SCE-MJ algorithm are also presented in Table 1. And the evolving processes of each algorithm on different test functions are shown in Figure 2.

The results presented in Table 1; Figure 2 align closely with previous studies conducted by Duan et al., in 1993 and Muttil and Jayawardena in 2008. It is worth noting that the FASCE algorithm demonstrates a remarkable ability to minimize failures and the number of function evaluations, particularly for the Rastrigin and Goldstein-Price functions, when compared to the original SCE-UA and SCE-MJ methods. Besides, the results show that the performance of FASCE is better than SCE-UA and SCE-MJ on two out of three 10-D functions. Although all the three algorithms cannot reach the global optimum on the 10-D Rosenbrock Function, the algorithm FASCE and SCE-MJ can significantly reduce the number functions estimations with the same search accuracy.

TABLE 1 Performance comparison of the three algorithms on eight benchmark test functions.

Problems	Number of complexes	Population size	SCE-UA		SCE-MJ			FASCE	
			NF	NFE	θ	NF	NFE	NF	NFE
Rastrigin	2	10	78	413	0.4	8	177	4	132
Goldstein-Price	2	10	0	162	0.5	0	81	0	65
Rosenbrock	2	10	9	335	0.2	3	262	1	211
Six-hump	2	10	8	178	0.5	0	76	0	75
Griewank	2	10	99	342	0.5	8	151	4	127
Rastrigin(10D)	10	200	4	10,085	0.4	1	3,017	1	2,162
Rosenbrock(10D)	10	200	100	10,248	0.2	100	2,889	100	2,177
Griewank(10D)	10	200	0	10,153	0.5	0	2,553	0	1,285

Note: The NF, denotes the number of failures out of 100 trials. The NFE, denotes the the number of function evaluations of the successful trials.

This indicates that the FASCE gets better performance than SCE-MJ and SCE-UA.

4 Hydrological model parameter calibration results based on FASCE

4.1 Parameter calibration of the hydrological model based on SVM

In this paper, we conducted a study on the Changjiang (Yangtze) River basin. To calibrate and validate our model, we used the observed streamflow data from Yichang Station between 1 January 2005, and 31 December 2007. The data is divided into two sets: the first 730 streamflow data points were used for model calibration, and the remaining data points were used for model validation.

Before we could begin calibrating our model, it was crucial to select an appropriate model structure. In this study, the SVM is chosen for one-day-ahead streamflow forecasting. This means that our model focuses on predicting future streamflow. We used the streamflow data from the past few days as inputs for the model, which is a common approach in similar studies (Aqil et al., 2007; Kisi, 2009; Wang et al., 2009). To determine which previous flow values to include as inputs, we utilized autocorrelation function (ACF) and partial autocorrelation function (PACF) analyses. You can find the ACF and PACF plots of the streamflow data in Figure 3.

Examining the results shown in Figure 3, it can be noted that:

1) The ACF exhibited a correlation coefficient higher than 0.8 at lag 5.
2) Additionally, the PACF showed significant correlation within a 95% confidence level interval for flow lags of up to 5 days.

Based on these findings, we concluded that the 5 antecedent flow values serve as suitable inputs for our daily streamflow forecasting model.

Here, the SVM algorithm is employed for streamflow forecasting. The primary objective (as Eq. 13) of using SVM is to discover a function that can accurately predict streamflow. SVM works by identifying a mathematical function that maps the input variables to the output variable, in this case, the streamflow.

By incorporating SVM into our approach, we can better forecast future streamflow levels, providing valuable insights for water resource management and planning.

$$\max\left[\sum_{i=1}^{l}(\alpha_i{}^{+}-\alpha_i{}^{-})y_i-\varepsilon\sum_{i=1}^{l}(\alpha_i{}^{+}+\alpha_i{}^{-})-\frac{1}{2}\sum_{i,j}(\alpha_i{}^{+}-\alpha_i{}^{-})\left(\alpha_j{}^{+}-\alpha_j{}^{-}\right)K\left(X_i,X_j\right)\right] \tag{13}$$

Subject to:

$$0\le\alpha_i^{+}\le C, 0\le\alpha_i^{-}\le C$$
$$\sum_{i=1}^{l}(\alpha_i^{+}-\alpha_i^{-})=0$$
$$i=1,2,\ldots,l$$

Where the $K(X_i, X_j)$ is the Kernel Trick, e.g., if the kernel function is Radial Basis Kernel, then $K(X_i, X_j) = \exp(-\frac{\|X_i-X_j\|^2}{2\sigma^2})$. C is the penalty factor. ε is the tolerance coefficient. σ is the kernel parameter. α^{+} and α^{-} are Lagrange coefficients.

The utilized equations clearly demonstrate that within the SVM-based model for daily streamflow prediction, there exist three specific parameters: the penalty factor C, tolerance level ε, and the kernel parameter σ. It's crucial that these parameters are accurately calibrated. Illustrating the varying ranges of parameters, Table 2 reflects the same parameter values as stipulated in the study by Gill et al., in 2006.

Furthermore, the model's training objective is primarily based on the Root Mean Square Error (RMSE), a statistically significant metric devised to quantify prediction error. The mathematical expression defining RMSE is demonstrated in the equation presented as Eq. 14.

$$\mathrm{RMSE}=\sqrt{\frac{1}{n}\sum_{i=1}^{n}\left(Q_{fore}^{i}-Q_{meas}^{i}\right)^2} \tag{14}$$

Where n denotes the length of streamflow; Q_{fore}^{i} denotes the ith forecasting streamflow value; Q_{meas}^{i} denotes the ith measured streamflow value.

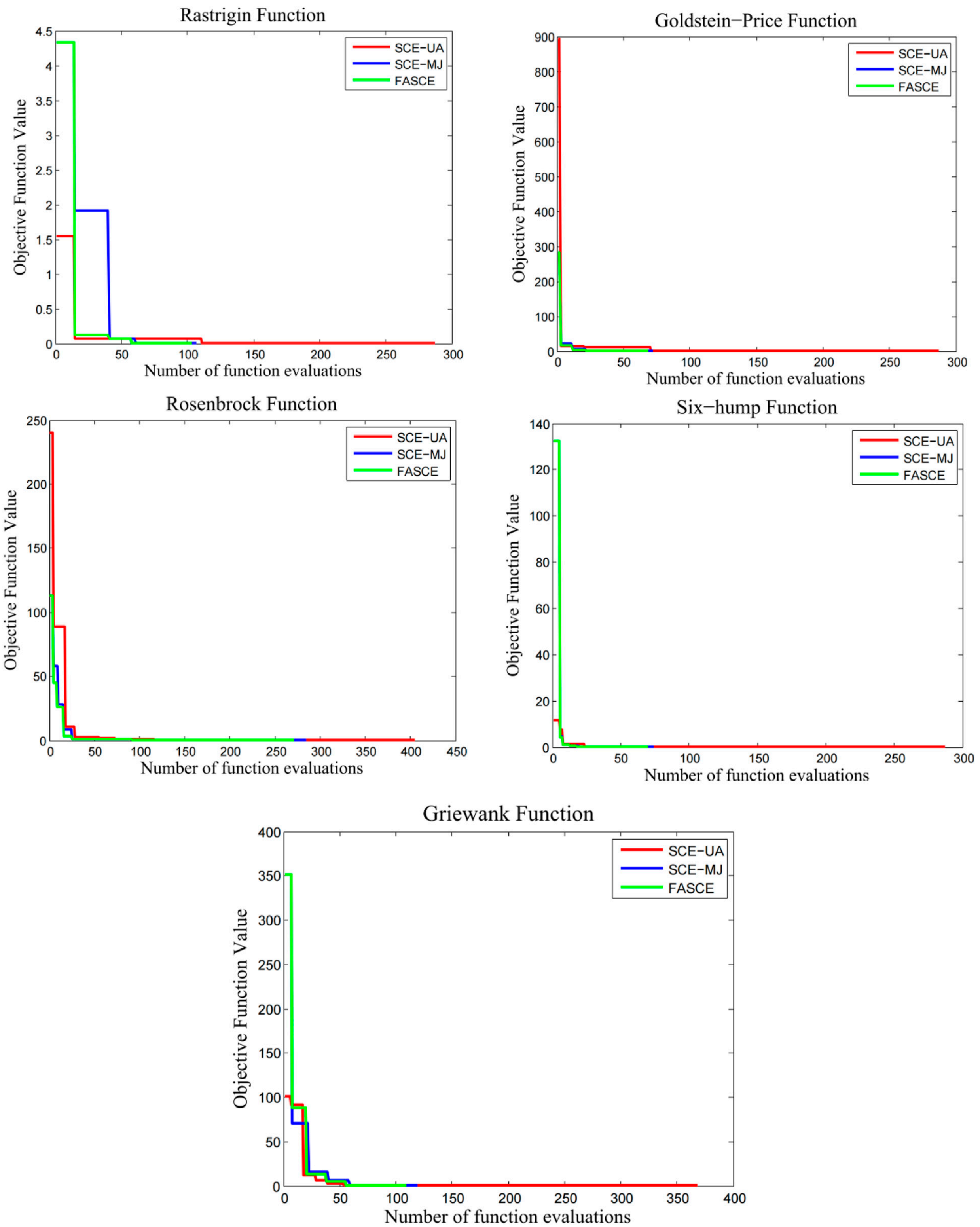

FIGURE 2
The evolving processes of each algorithm on different test functions.

A series of test trials are executed prior to initiating the actual training phase, with the primary goal of identifying the optimal success threshold. The model has undergone several iterations of preliminary testing, leading to the observation that the optimal RMSE value achieved via the FASCE algorithm is approximately 3,270 m^3/s. Hence, this specific value is assigned as the success threshold determinant. In essence, a trial is considered successful if the best function value yielded by the algorithm is less than

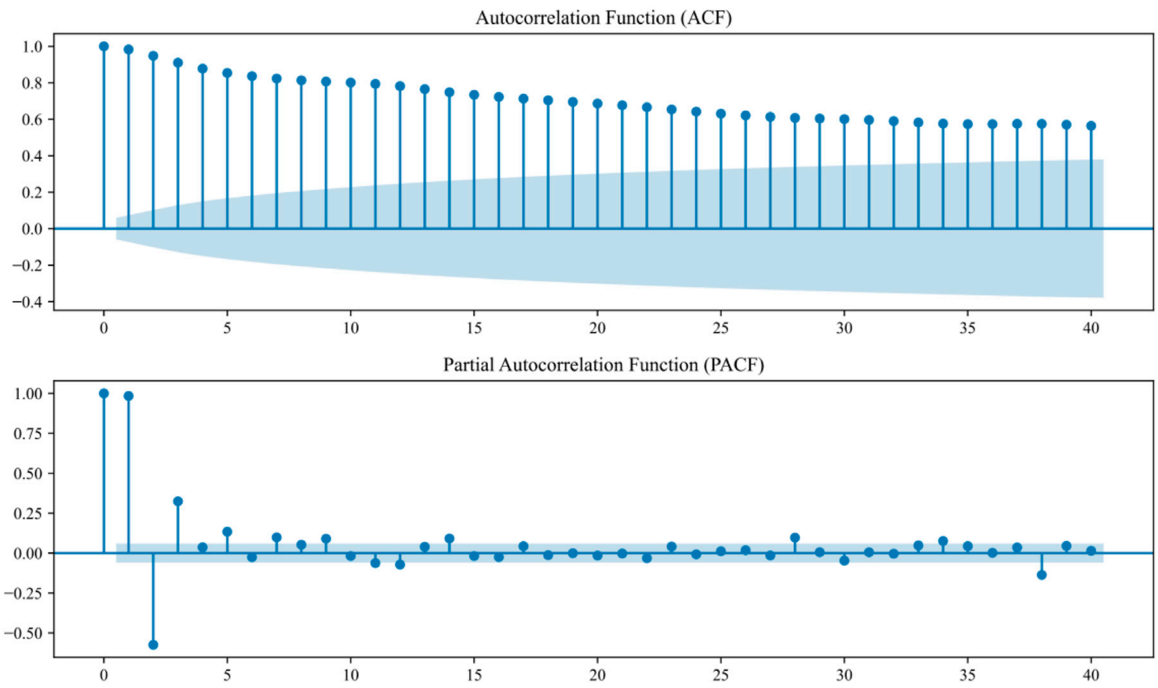

FIGURE 3
The ACF and PACF plots of the streamflow data.

TABLE 2 The detail of the SVM parameters.

Parameters name	Range
Penalty coefficient C	40.25–43.10
Kernel parameter σ	0.001–0.009
Tolerance ε	0.12–0.14

TABLE 3 The mean forecasting performance of 20 trials for each algorithm on SVM based hydrological model calibration.

Algorithms	Calibration		Validation	
	RMSE (m^3/s)	ME (m^3/s)	RMSE (m^3/s)	ME (m^3/s)
SCE-UA	3,874	2,218	4,145	2,368
SCE-MJ	2,993	1,939	3,410	1,983
FASCE	2,774	1860	3,311	1,935

3,270 m^3/s. On the contrary, a trial is deemed a failure if it hits the maximum limit of function evaluations. To moderate the potential impact of any inherent random element within the previously discussed three algorithms, each one is operated independently 20 times. The experimental outcomes are consolidated and presented in Tables 3, 4.

Within the context of this paper, two key metrics have been selected as the estimate indices for forecasting results: the Root Mean Square Error (RMSE) and Mean Error (ME). ME can be calculated by Eq. 15. The mathematical interpretation of ME is explained in the subsequent equation. Lower RMSE and ME values are indicative of superior performance.

$$\mathrm{ME} = \frac{1}{n}\sum_{i=1}^{n}\left|Q_{fore}^{i} - Q_{meas}^{i}\right| \tag{15}$$

Where n denotes the length of streamflow; Q_{fore}^{i} denotes the ith forecasting streamflow value; Q_{meas}^{i} denotes the ith measured streamflow value.

Based on the analysis shown in Table 3, it is evident that three algorithms exhibit nearly identical RMSE values, thereby indicating the suitability of the threshold value of 3,270 m^3/s. To further evaluate the efficiency of these algorithms, Table 4 provides a summary of their performance. Clearly, the FASCE algorithm outperforms the other two algorithms in terms of achieving the same level of performance. Not only does FASCE demonstrate significantly faster speed compared to SCE-UA and SCE-MJ, but it also exhibits similar search accuracy when compared to SCE-MJ. One possible reason for this could be that the FASCE algorithm primarily focuses on enhancing the search speed of SCE-MJ, without modifying its local searching operator.

Figure 4 illustrates the results obtained by the FASCE algorithm during the calibration and validation period. In this figure, dots represent the observed streamflow, while lines represent the predicted streamflow. It is worth noting that the model accurately captures the characteristics of the streamflow hydrograph, although some timing errors are present. This indicates that there may be a need for further improvement in the model structure.

TABLE 4 The efficient performance of each algorithm on SVM based hydrological model calibration.

Algorithms	Min	Max	Mean	<100	NF
SCE-UA	112	576	304	0	4
SCE-MJ	91	912	226	3	0
FASCE	58	475	195	6	0

Note: Min denotes the minimum number of the model evaluations among the 20 independent trials, Max denotes the maximum number of the model evaluations among the 20 independent trials, Mean denotes the mean number of model evaluations of the 20 independent trials, and <100 denotes the count of trials with number of model evaluations below 100, and NF, denotes the number of failure trials among the 20 independent trials.

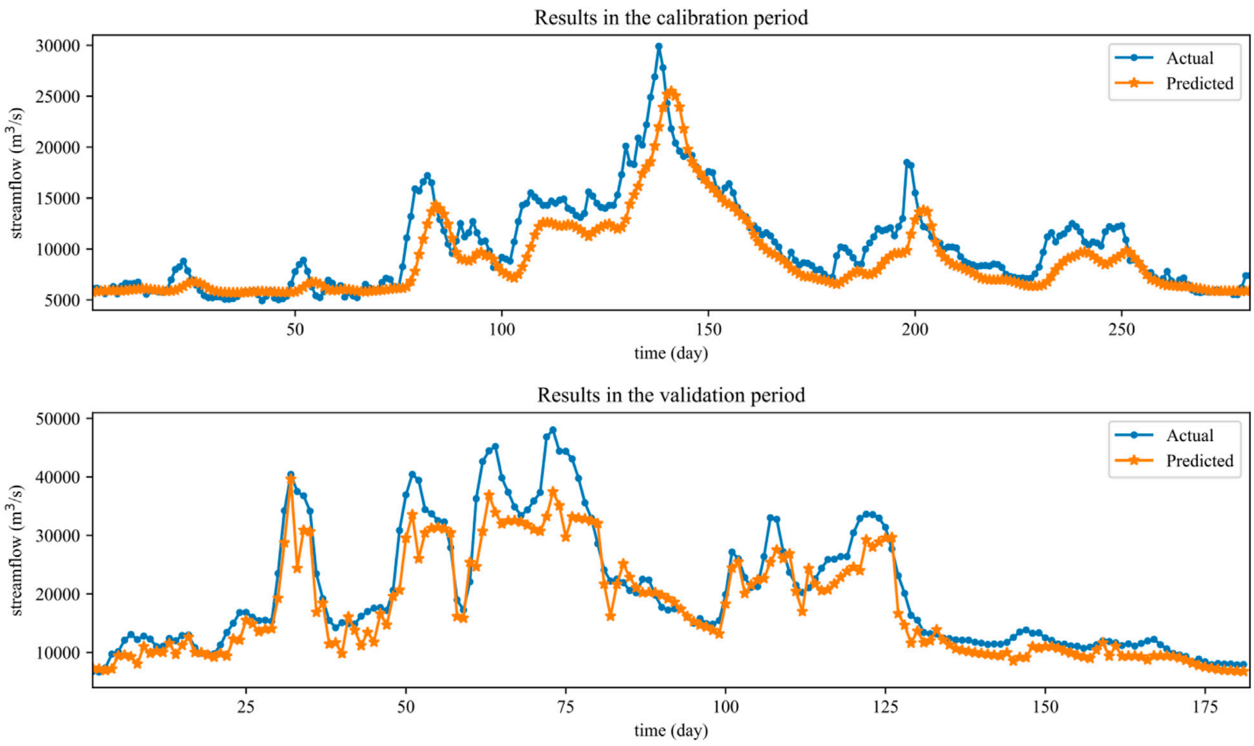

FIGURE 4
Streamflow forecasting results during calibration period and validation period with FASCE algorithm.

4.2 Parameter calibration of the Xinanjiang hydrological model

Xinanjiang model is first proposed by Professor Zhao Renjun in China. This model is widely used in streamflow prediction in moist and semi-humid basins. The most widely used framework is the three source Xinanjiang model. And the parameter descriptions are shown in Table 5. The basic frame and the description of the model parameters can be referred to the references (Zhao, 1992; Li et al., 2009; Song et al., 2012; Rahman and Lu, 2015).

In this research, the streamflow prediction of Zishui watershed is taken as the second case study. The Zishui watershed area is about 22,640 km^2, and this watershed plays an important role in power generation and flood control in Hunan province. The location of the Zishui watershed is shown as Figure 5.

The Zishui watershed has 32 rainfall stations, 6 water level stations. The history of water and rainfall observation data of river basin is very complete. The observed data from the 32 rainfall stations and 6 water level stations between 2004-1-1 and 2014-12-31 is used for model calibration and validation. The observation data for the first 6 years is used for model calibration, while the rest used for model validation.

Three algorithms SCE-UA, SCE-UA-MJ and FASCE are employed for model calibration. Similar with the above case study, the Root Mean Square Error (RMSE) is selected as the training objective function. From several forwards testing of the model, we note that the best RMSE value found by FASCE algorithm is about 662 m^3/s. Therefore, this value 662 m^3/s is selected as a threshold to determine a trial is success or not. To reduce the influence of the random factor existed in the above mentioned three algorithms, each algorithm runs 20 times independently. The results of the experiment are summarized in Tables 6, 7.

The model parameter calibration results of the FASCE are shown in Table 8.

The results obtained by FASCE algorithm in calibration and validation period are given in Figure 6, where dots denote the

TABLE 5 The parameters of the Xinanjiang model.

Parameter	Range	Physical description
U_m(mm)	5–20 mm	Upper tension water capacity
L_m(mm)	60–90 mm	Lower tension water capacity
D_m(mm)	15–60 mm	Deep tension water capacity
B	0.1–0.4	Tension water storage capacity curve factor
I_m(%)	0–0.03	Impervious area ratio
K	0.5–1.1	Conversion coefficient of evaporation capacity
C	0.08–0.18	Coefficient of deep evaporation
S_m(mm)	10–50 mm	Free water storage capacity
E_x	0.5–2.0	Free water storage capacity curve factor
K_g	0.35–0.45	Outflow coefficient of free water reservoir to groundwater reservoir
K_i	0.25–0.35	Outflow coefficient of free water reservoir to interflow reservoir
C_g	0.99–0.998	Recession coefficient of groundwater reservoir
C_i	0.5–0.9	Recession coefficient of interflow
C_s	0.01–0.5	Recession coefficient of river network water storage capacity
K_e	0.1–1	Parameter of muskingum method
X_e	0–0.5	Parameter of muskingum method
L	Empirical value	The confluence time of river network
N	Empirical value	Lengths of flow confluence

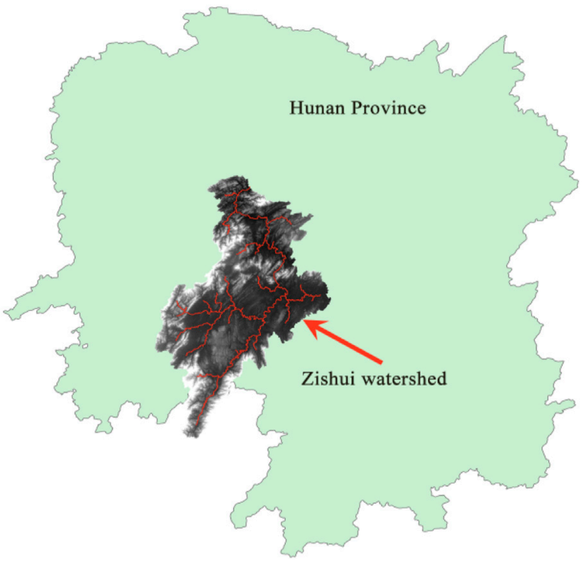

FIGURE 5
The location of the Zhexi reservoir watershed.

observed streamflow while lines denote the predicted streamflow. It can also be indicated that the model can fit the characteristics of the streamflow hydrograph very well.

TABLE 6 The mean forecasting performance of 20 trials for each algorithm on Xinanjiang hydrological model calibration.

Algorithms	Calibration		Validation	
	RMSE(m^3/s)	ME(m^3/s)	RMSE(m^3/s)	ME(m^3/s)
SCE-UA	757	678	818	575
SCE-MJ	534	433	645	527
FASCE	482	305	556	434

From the above results, it can be noted that three algorithms can all get very good performance, and the algorithm FASCE are more efficient to arrive at the same performance than the other two algorithms. Same with the above case study, the FASCE mainly enhances the evolving speed, so the FASCE has faster converge speed but nearly same search accuracy than SCE-MJ.

5 Conclusion

In this paper, we introduce an exciting new algorithm called FASCE that aims to enhance model parameter calibration. The FASCE algorithm builds upon the foundation of the original SCE-UA algorithm by implementing a modified adaptive simplex search and incorporating a new strategy for locating the initial population. The effectiveness of the FASCE algorithm is tested on eight

TABLE 7 The efficient performance of each algorithm on Xinanjiang hydrological model calibration.

Algorithms	Min	Max	Mean	NF
SCE-UA	481	1,312	655	2
SCE-MJ	325	1,087	563	0
FASCE	218	709	377	0

Note: Min denotes the minimum number of the model evaluations among the 20 independent trials, Max denotes the maximum number of the model evaluations among the 20 independent trials, Mean denotes the mean number of model evaluations of the 20 independent trials, and NF, denotes the number of failure trials among the 20 independent trials.

TABLE 8 The calibration results of the Xinanjiang model.

Parameter	UM	LM	DM	B	IM	K	C	SM
Value	46.46	61.45	15.32	0.54	0.001	1.03	0.20	44.81
Parameter	EX	KI	KG	CI	CG	CS	KE	XE
Value	0.5	0.19	0.25	0.5	0.99	0.81	0.74	0.37

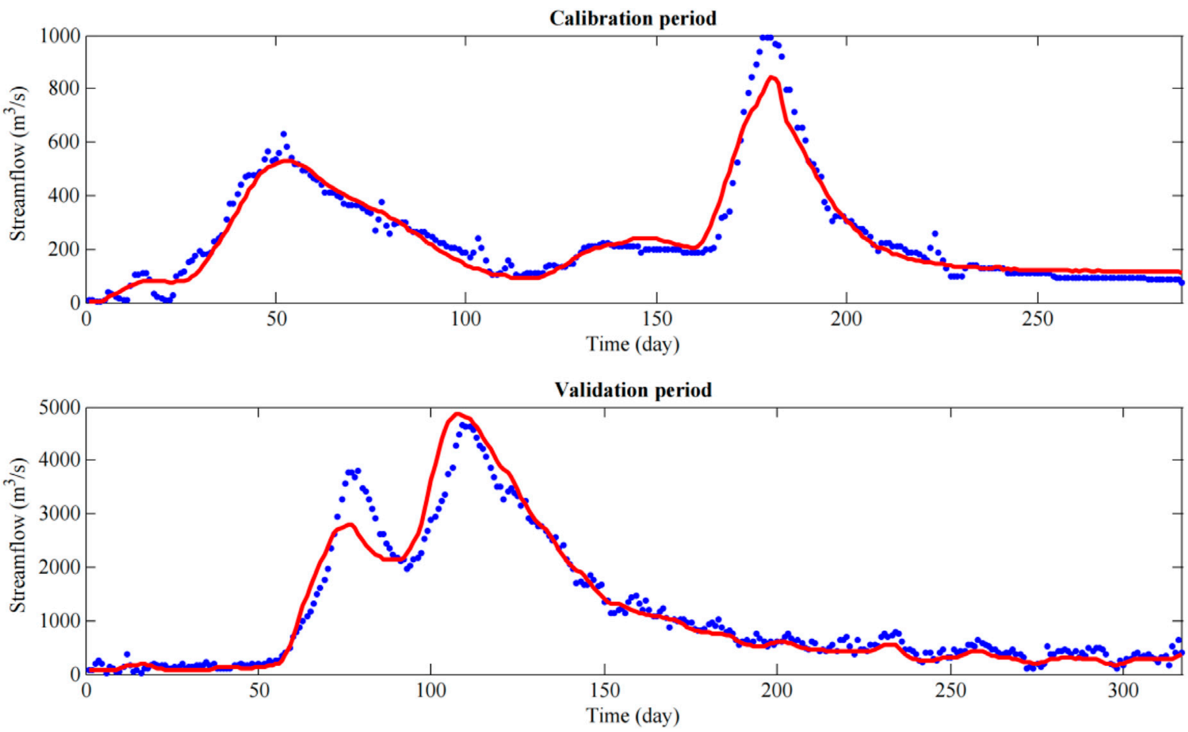

FIGURE 6
Streamflow forecasting results of the Zishui watershed during calibration period and validation period with FASCE algorithm.

benchmark functions and two daily streamflow forecasting model based on SVM and Xinanjiang model. The results are then compared with those achieved using the original SCE-UA algorithm and SCE-MJ algorithm. Based on our findings, the following conclusions can be drawn:

1) The FASCE algorithm introduces an adaptive shuffle operator, which greatly improves the convergence speed of SCE-UA. By dynamically shifting the newly generated points towards the best point found so far, a significant enhancement can be noted in convergence speed across various test functions and two hydrological forecasting models.
2) Setting a proper shift coefficient in advance for the SCE-MJ algorithm is a challenging task. Additionally, using a constant shift coefficient throughout the entire evolutionary computation process seems impractical. To address these limitations, we propose the novel FASCE algorithm, which includes an adaptive shift operator. This operator does not require any

predefined parameters and adjusts the shift coefficient based on the evolving population characteristics during the computation process. This innovative design overcomes the shortcomings of SCE-MJ and significantly improves the algorithm's convergence performance.

3) Initial tests were conducted on a set of functions to assess FASCE's efficacy. The results showed that FASCE could curtail the failure rate by a minimum of 80%, whereas the requirement for function evaluations fell between 30% and 60%. Two hydrological models - SVM and Xinanjiang rainfall-runoff model were employed to estimate the new algorithm's performance. No failures were reported, and there was a reduction of at least 30% in function evaluations using FASCE.
4) While the FASCE algorithm demonstrates excellent performance overall, it may yield suboptimal results in specific problem scenarios. As a result, we plan to focus our future work on enhancing the algorithm's search capability for high-dimensional problems.

Data availability statement

The original contributions presented in the study are included in the article/Supplementary Material, further inquiries can be directed to the corresponding author.

Author contributions

JL: Conceptualization, Funding acquisition, Project administration, Writing–original draft, Writing–review and editing. HH: Conceptualization, Writing–review and editing. WF: Methodology, Visualization, Writing–review and editing. YC: Software, Validation, Writing–review and editing.

Funding

The author(s) declare financial support was received for the research, authorship, and/or publication of this article. This research work is support by the Science and Technology Project of China Southern Power Grid Co., Ltd., (GDKJXM20220232).

Acknowledgments

Thanks to the editorial team and the reviewers for their valuable feedback and assistance in improving our article.

Conflict of interest

Authors JL, HH, WF, and YC were employed by Guangdong Power Grid Co., Ltd.

Publisher's note

References

Ajami, N. K., Gupta, H., Wagener, T., and Sorooshian, S. (2004). Calibration of a semi-distributed hydrologic model for streamflow estimation along a river system. *J. Hydrology* 298 (1-4), 2–35. doi:10.1016/j.jhydrol.2004.03.033

Aqil, M., Kita, I., Yano, A., and Nishiyama, S. (2007). A comparative study of artificial neural networks and neuro-fuzzy in continuous modeling of the daily and hourly behaviour of runoff. *J. Hydrology* 337 (1-2), 22–34. doi:10.1016/j.jhydrol.2007.01.013

Bremermann, H. J., Rogson, M., and Salaff, S. (1966). in *Global properties of evolutionprocesses. Natural automata and useful simulations*. Editors H. H. Pattee, E. A. Edelsack, L. Feinand, and A. B. Callahan (Washington D.C.: Spartan Books), 3–41.

Brunetti, G., Stumpp, C., and Šimůnek, J. (2022). Balancing exploitation and exploration: a novel hybrid global-local optimization strategy for hydrological model calibration. *Environ. Model. Softw.* 150, 105341. doi:10.1016/j.envsoft.2022.105341

Chen, L., Singh, V. P., and Guo, S. (2013). Measure of correlation between river flows using the copula-entropy method. *J. Hydrologic Eng.* 18 (12), 1591–1606. doi:10.1061/(asce)he.1943-5584.0000714

Chen, L., Singh, V. P., Lu, W., Zhang, J., Zhou, J., and Guo, S. (2016). Streamflow forecast uncertainty evolution and its effect on real-time reservoir operation. *J. Hydrology* 540, 712–726. doi:10.1016/j.jhydrol.2016.06.015

Chu, W., Yang, T., and Gao, X. (2014). Comment on 'High-dimensional posterior exploration of hydrologic models using multiple-try DREAM (ZS) and high-performance computing' by Eric Laloy and Jasper A. Vrugt. *Water Resour. Res.* 50 (3), 2775–2780. doi:10.1002/2012wr013341

Deng, C., Liu, P., Liu, Y., Wu, Z., and Wang, D. (2015). Integrated hydrologic and reservoir routing model for real-time water level forecasts. *J. Hydrologic Eng.* 20 (9), 05014032. doi:10.1061/(asce)he.1943-5584.0001138

Duan, Q., and Gupta, V. K. (1993). Shuffled complex evolution approach for effective and efficient global minimization. *J. Optim. Theory Appl.* 76 (3), 501–521. doi:10.1007/bf00939380

Duan, Q., Sorooshian, S., and Gupta, V. (1992). Effective and efficient global optimization for conceptual rainfall-runoff models. *Water Resour. Res.* 28 (4), 1015–1031. doi:10.1029/91wr02985

Fogel, G. B., Andrews, P. C., and Fogel, D. B. (1998). On the instability of evolutionary stable strategies in small populations. *Ecol. Modell.* 109 (3), 283–294. doi:10.1016/S0304-3800(98)00068-4

Galar, R. (1985). Handicapped individuals in evolutionary processes. *Biol. Cybern.* 51 (1), 1–9. doi:10.1007/BF00355685

Gill, M. K., Kaheil, Y. H., Khalil, A., McKee, M., and Bastidas, L. (2006). Multiobjective particle swarm optimization for parameter estimation in hydrology. *Water Resour. Res.* 42, W07417. doi:10.1029/2005wr004528

Gopala, S. P., Kawamura, A., Amaguchi, H., Takasaki, T., and Azhikodan, G. (2019). A bootstrap approach for the parameter uncertainty of an urban-specific rainfall-runoff model. *J. Hydrology* 579, 124195. doi:10.1016/j.jhydrol.2019.124195

Guo, J., Liu, Y., Zou, Q., Ye, L., Zhu, S., and Zhang, H. (2023). Study on optimization and combination strategy of multiple daily runoff prediction models coupled with physical mechanism and LSTM. *J. Hydrology* 624, 129969. doi:10.1016/j.jhydrol.2023.129969

Hallabia, H., Hamam, H., and Ben Hamida, A. (2021). An optimal use of SCE-UA method cooperated with superpixel segmentation for pansharpening. *IEEE Geoscience Remote Sens. Lett.* 18, 1620–1624. doi:10.1109/lgrs.2020.3004320

He, B., Takase, K., and Wang, Y. (2007). Regional groundwater prediction model using automatic parameter calibration SCE method for a coastal plain of Seto Inland Sea. *Water Resour. Manag.* 21 (6), 947–959. doi:10.1007/s11269-006-9066-7

Her, Y., and Heatwole, C. (2016). Two-dimensional continuous simulation of spatiotemporally varied hydrological processes using the time-area method. *Hydrol. Process.* 30 (5), 751–770. doi:10.1002/hyp.10644

Jiang, C., Zhang, S., and Xie, Y. (2023). Constrained shuffled complex evolution algorithm and its application in the automatic calibration of Xinanjiang model. *Front. Earth Sci.* 10, 1037173. doi:10.3389/feart.2022.1037173

Kisi, O. (2009). Neural networks and wavelet conjunction model for intermittent streamflow forecasting. *J. Hydrologic Eng.* 14 (8), 773–782. doi:10.1061/(asce)he.1943-5584.0000053

Kisi, O., and Cimen, M. (2011). A wavelet-support vector machine conjunction model for monthly streamflow forecasting. *J. Hydrology* 399 (1-2), 132–140. doi:10.1016/j.jhydrol.2010.12.041

Li, H. X., Zhang, Y. Q., Chiew, F. H. S., and Xu, S. G. (2009). Predicting runoff in ungauged catchments by using Xinanjiang model with MODIS leaf area index. *J. Hydrology* 370 (1-4), 155–162. doi:10.1016/j.jhydrol.2009.03.003

Li, Q., and Ouyang, S. (2015). Research on multi-objective joint optimal flood control model for cascade reservoirs in river basin system. *Nat. Hazards* 77 (3), 2097–2115. doi:10.1007/s11069-015-1692-z

Li, Z., Xin, P., and Tang, J. (2013). Study of the Xinanjiang model parameter calibration. *J. Hydrologic Eng.* 18 (11), 1513–1521. doi:10.1061/(asce)he.1943-5584.0000527

Lin, J. Y., Cheng, C. T., and Chau, K. W. (2006). Using support vector machines for long-term discharge prediction. *Hydrological Sci. J.* 51 (4), 599–612. doi:10.1623/hysj.51.4.599

Liu, H., Zhao, W., He, Z., and Liu, J. (2015). Soil moisture dynamics across landscape types in an arid inland river basin of Northwest China. *Hydrol. Process.* 29 (15), 3328–3341. doi:10.1002/hyp.10444

Mao, Y., Zhang, X., and Li, Z. (2013). Coupled simulation of Xinanjiang model with MODFLOW. *J. Hydrologic Eng.* 18 (11), 1443–1449. doi:10.1061/(asce)he.1943-5584.0000706

Mcmillan, H., Freer, J., Pappenberger, F., Krueger, T., and Clark, M. (2010). Impacts of uncertain river flow data on rainfall-runoff model calibration and discharge predictions. *Hydrol. Process.* 24 (10), 1270–1284. doi:10.1002/hyp.7587

Mohsen, B., Keyvan, A., Morteza, E., and Palhang, M. (2009). Generalization performance of support vector machines and neural networks in runoff modeling. *Expert Syst. Appl.* 36 (4), 7624–7629. doi:10.1016/j.eswa.2008.09.053

Muttil, N., and Jayawardena, A. W. (2008). Shuffled Complex Evolution model calibrating algorithm: enhancing its robustness and efficiency. *Hydrol. Process.* 22 (23), 4628–4638. doi:10.1002/hyp.7082

Muttil, N., and Liong, S. Y. (2004). Superior exploration–exploitation balance in shuffled complex evolution. *J. Hydrologic Eng.* 130 (12), 1202–1205. doi:10.1061/(asce)0733-9429(2004)130:12(1202)

Ouyang, S., Zhou, J., Zhou, C., and Wang, H. (2013). Research on impounding dispatch for the lower cascade reservoir in Jinsha River and Three Gorges cascade. *J. Hydraulic Eng.* 44 (4), 435–443. doi:10.13243/j.cnki.slxb.2013.04.009

Qin, H., Zhou, J., Lu, Y., Li, Y., and Zhang, Y. (2010). Multi-objective cultured differential evolution for generating optimal trade-offs in reservoir flood control operation. *Water Resour. Manag.* 24 (11), 2611–2632. doi:10.1007/s11269-009-9570-7

Rahman, M. M., and Lu, M. (2015). Model spin-up behavior for wet and dry basins: a case study using the Xinanjiang model. *Water* 7 (8), 4256–4273. doi:10.3390/w7084256

Santos, C. A. G., Srinivasan, V. S., Suzuki, K., and Watanabe, M. (2003). Application of an optimization technique to a physically based erosion model. *Hydrol. Process.* 17 (5), 989–1003. doi:10.1002/hyp.1176

Song, X. M., Kong, F. Z., Zhan, C. S., and Han, J. W. (2012). Hybrid optimization rainfall-runoff simulation based on Xinanjiang model and artificial neural network. *J. Hydrologic Eng.* 17 (9), 1033–1041. doi:10.1061/(asce)he.1943-5584.0000548

Tripathi, S., Srinivas, V. V., and Nanjundiah, R. S. (2006). Downscaling of precipitation for climate change scenarios: a support vector machine approach. *J. Hydrology* 330 (3-4), 621–640. doi:10.1016/j.jhydrol.2006.04.030

Tsai, M. J., Abrahart, R. J., Mount, N. J., and Chang, F. J. (2014). Including spatial distribution in a data-driven rainfall-runoff model to improve reservoir inflow forecasting in Taiwan. *Hydrol. Process.* 28 (3), 1055–1070. doi:10.1002/hyp.9559

Uniyal, B., Jha, M. K., and Verma, A. K. (2015). Parameter identification and uncertainty analysis for simulating streamflow in a river basin of Eastern India. *Hydrol. Process.* 29 (17), 3744–3766. doi:10.1002/hyp.10446

Wang, W., Chau, K., Cheng, C., and Qiu, L. (2009). A comparison of performance of several artificial intelligence methods for forecasting monthly discharge time series. *J. Hydrology* 374 (3), 294–306. doi:10.1016/j.jhydrol.2009.06.019

Xu, D., Wang, X., Wang, W., Chau, K. w., and Zang, H. f. (2023). Improved monthly runoff time series prediction using the SOA–SVM model based on ICEEMDAN–WD decomposition. *J. Hydroinformatics* 25, 943–970. doi:10.2166/hydro.2023.172

Yan, L., Lei, Q., Jiang, C., Yan, P., Ren, Z., Liu, B., et al. (2022). Climate-informed monthly runoff prediction model using machine learning and feature importance analysis. *Front. Environ. Sci.* 10, 1049840. doi:10.3389/fenvs.2022.1049840

Yang, J., McMillan, H., and Zammit, C. (2017a). Modeling surface water–groundwater interaction in New Zealand: model development and application. *Hydrol. Process.* 31 (4), 925–934. doi:10.1002/hyp.11075

Yang, T., Gao, X., Sellars, S. L., and Sorooshian, S. (2015). Improving the multi-objective evolutionary optimization algorithm for hydropower reservoir operations in the California Oroville-Thermalito complex. *Environ. Model. Softw.* 69 (C), 262–279. doi:10.1016/j.envsoft.2014.11.016

Yang, T., Tao, Y., Li, J., Zhu, Q., Su, L., He, X., et al. (2017b). Multi-criterion model ensemble of CMIP5 surface air temperature over China. *Theor. Appl. Climatol.* 2017 (6), 1057–1072. doi:10.1007/s00704-017-2143-4

Yapo, P., Gupta, V. K., and Sorooshian, S. (1996). Automatic calibration of conceptual rainfall-runoff models: sensitivity to calibration data. *J. Hydrology* 181 (1-4), 23–48. doi:10.1016/0022-1694(95)02918-4

Yazdi, J., Salehi Neyshabouri, S. A. A., and Golian, S. (2014). A stochastic framework to assess the performance of flood warning systems based on rainfall-runoff modeling. *Hydrol. Process.* 28 (17), 4718–4731. doi:10.1002/hyp.9969

Yoon, H., Jun, S. C., Hyun, Y., Bae, G. O., and Lee, K. K. (2010). A comparative study of artificial neural networks and support vector machines for predicting groundwater levels in a coastal aquifer. *J. Hydrology* 36 (4), 7624–7629. doi:10.1016/j.jhydrol.2010.11.002

Zhao, R. J. (1992). The Xinanjiang model applied in China. *J. Hydrology* 135 (1-4), 371–381. doi:10.1016/0022-1694(92)90096-e

Zhao, R. J., Liu, X. R., and Singh, V. P. (1995). The Xinanjiang model. *Proc Oxf. Symposium Hydrological Forecast. Iahs Publ* 135 (1), 371–381.

Zhou, J., Song, L., Kursan, S., and Liu, Y. (2015). A two-dimensional coupled flow-mass transport model based on an improved unstructured finite volume algorithm. *Environ. Res.* 139, 65–74. doi:10.1016/j.envres.2015.01.017